DISCRETE WAVELET PACKET BASED MULTITONE MODULATION FOR TRANSMITTING COMPLEX SYMBOLS

T.K. Adhikary and V.U. Reddy
Department of Electrical Communication Engineering,
Indian Institute of Science, Bangalore-560012, India.

ABSTRACT

Multicarrier modulation (MCM) methods have been attracting considerable attention lately. In this paper, we address MCM techniques based on wavelet packets for QAM (quadrature amplitude modulation) and PM (phase modulation) symbol constellations. We first discuss the design of complex wavelet packets, which serve as orthonormal carriers for MCM, and then describe a DWMT (discrete wavelet multitone) scheme for transmitting QAM and PM symbols. We consider both blind and non-blind schemes for retrieving the symbols at the receiver. Simulations have been carried out to study the performance with both the schemes.

1 INTRODUCTION

Recently, multicarrier modulation (MCM) schemes have been attracting a lot of attention. In MCM, the channel is partitioned into a number of subchannels and each of which is assigned a distinct carrier. These carriers are orthogonal to each other.

The discrete multitone (DMT) modulation, a DFT based MCM technique, can be implemented with FFT algorithm thereby achieving substantial reduction in computation. But, the amplitude responses of the Fourier transform of the DFT bases have high degree of spectral overlap among themselves. On the other hand, discrete wavelet multitone (DWMT) modulation system uses wavelet packet bases, which can be designed to achieve high level of spectral containment.

The DWMT system for PAM symbol constellations is described in [2]. In this paper, we address DWMT system for QAM and PM symbol constellations. We first discuss the design of complex wavelet packet bases and then describe the DWMT scheme. We also extend a recently proposed DWMT technique with blind equalization [8] to QAM, PM and higher order PAM symbol constellations.

Notation: Bold faced upper and lower case letters denote matrices and vectors, respectively. $\mathbf{A}^T$, $\mathbf{A}^*$ and $\mathbf{A}^\dagger$ represent transpose, conjugate and conjugate-transpose of $\mathbf{A}$. $\tilde{\mathbf{H}}(z) = \mathbf{H}^\dagger(1/z^*)$, $\mathbf{I}$ is the identity matrix, $x(n) * y(n)$ denotes convolution of $x(n)$ and $y(n)$, and $F(z)$ is z-transform of $f(n)$, $j = \sqrt{-1}$. $\delta(n)$ is the unit impulse function.

2 DESIGN OF COMPLEX BASES

Any complex multicarrier bases, to be used for MCM, should exhibit the desired orthogonality. Further, the real and imaginary parts of the complex bases should be spectrally similar and also orthogonal to each other. One such design method based on combined sine and cosine modulation has been described in [3]. However, the design contains too many constrains resulting in poorer stopband attenuation. Here we discuss Method 1 design only and refer to [6] for Method 2 design.

2.1 Method 1

We first design an M-band cosine modulated filter bank [1] $\mathbf{h}'^T(z) = [H'_0(z)\ H'_1(z)\ \cdots\ H'_{M-1}(z)]$. Let $\mathbf{E}'(z)$ denote the polyphase matrix of the filter bank. Then $\mathbf{h}'(z) = \mathbf{E}'(z)\mathbf{e}(z)$ where $\mathbf{e}^T(z) = [1\ z^{-1} \cdots z^{-M+1}]$. The cosine modulated filters are orthogonal since $\mathbf{E}'(z)$ is paraunitary [1].

Here, we consider the case for M even. To get a pair of bases in the same band, we generate a modified filter bank $\mathbf{h}^{\iota T}(z) = [H^\iota_0(z)\ H^\iota_1(z)\ \cdots\ H^\iota_{M-1}(z)]$ as

$$\mathbf{h}^\iota(z) = \frac{1}{\sqrt{2}}\mathbf{R}\mathbf{h}'(z) = \frac{1}{\sqrt{2}}\mathbf{R}\mathbf{E}'(z)\mathbf{e}(z) \tag{1}$$

where

$$\mathbf{R} = \begin{bmatrix} 1 & 1 & 0 & 0 & \cdots & 0 \\ 1 & -1 & 0 & 0 & \cdots & 0 \\ 0 & 0 & 1 & 1 & \cdots & 0 \\ 0 & 0 & 1 & -1 & \cdots & 0 \\ . & . & . & . & \cdots & . \end{bmatrix} \tag{2}$$

The polyphase matrix of the new filter bank, $\mathbf{E}^\iota(z)$, is $\frac{1}{\sqrt{2}}\mathbf{R}\mathbf{E}'(z)$. Since $\mathbf{R}^T\mathbf{R} = 2\mathbf{I}$, $\tilde{\mathbf{E}}^\iota(z)\mathbf{E}^\iota(z) = \mathbf{I}$. Thus, $\mathbf{E}^\iota(z)$ is paraunitary.

The bandwidth of the modified filters is twice that of the original cosine modulated filters. They are spectrally similar in pairs, at least in the passband. From the filters so generated, we form the complex impulse responses of the analysis bank filters by choosing the impulse responses of a pair of filters in the same band as the real and imaginary parts. We thus obtain $M/2$ complex filters from M-band cosine modulated filter bank. The impulse responses of the other $M/2$ complex filters are the complex conjugates of the first set of $M/2$ filters designed as above. Thus, the impulse responses of the M complex analysis filters are

$$\begin{aligned} h_k(n) &= \frac{1}{\sqrt{2}}h^\iota_{2k}(n) + j\frac{1}{\sqrt{2}}h^\iota_{2k+1}(n) \\ h_{M-1-k}(n) &= \frac{1}{\sqrt{2}}h^\iota_{2k}(n) - j\frac{1}{\sqrt{2}}h^\iota_{2k+1}(n) \end{aligned} \tag{3}$$

for $0 \le k \le M/2 - 1$ and $0 \le n \le L_1 - 1$, where L_1 is the length of the prototype filter.

The impulse responses of the corresponding synthesis filters are given by

$$f_k(n) = h_k^*(L_1 - 1 - n), \quad 0 \le k \le M-1 \text{ and } 0 \le n \le L_1 - 1. \tag{4}$$

We refer to these responses as the complex wavelet packet bases, which constitute the carriers for multicarrier modulation. They satisfy the orthogonality relation

$$\sum_n f_k(n) f_l^*(n + iM) = \delta(k-l)\delta(i), \quad 0 \le k, l \le M-1. \tag{5}$$

3 DWMT Modulation SYSTEM

In this section, we describe the multicarrier system for transmitting QAM and PM symbols.

3.1 A Discrete Multicarrier System

Consider the multicarrier system shown in Fig. 1. $C(z)$ and $W(z)$ represent the channel and the pre-detection equalizer, respectively. $\{f_m(n)\}$ correspond to IDFT bases for the DMT case and complex wavelet packet bases for the DWMT case. Let N be the length of the bases. Then $N = L_1$ for DWMT bases and $N = M$ for IDFT bases. In the case of DMT, $pM = M$, i.e., $p = 1$, and in DWMT $pM = L_1$. The m^{th} filter in the receiver is given by $F_m'(z) = z^{-d-N}\tilde{F}_m(z)$, where $\tilde{F}_m(z) = F_m^*(1/z^*)$. Let $B(z) = z^{-D}B'(z)$ be the minimum mean square error estimate of $C(z)W(z)$ and Δ be the nominal delay introduced by $B'(z)$. Then, $d = KM - D - \Delta$ where K is chosen to make d non-negative so that the receiver filters are causal. From the above choice of the modulator and demodulator filters, their impulse responses are related as

$$f_m'(n) = f_m^*(N + d - n), \quad d+1 \le n \le N+d \tag{6}$$

and $f_m'(n) = 0$ otherwise. The modulator filters satisfy the orthogonality relation

$$\sum_{n=-\infty}^{+\infty} f_{m_1}(n) f_{m_2}^*(n + lM) = \delta(l)\delta(m_1 - m_2). \tag{7}$$

Similar relation holds for the demodulator filters also.

$x_m(n)$ represents the input symbol in the n^{th} block that is to be transmitted on m^{th} carrier. To get a real output from the multicarrier modulator in the DMT case, the symbols in a block should satisfy the relation $x_{M-m}(n) = x_m^*(n) \quad 0 < m < \frac{M}{2}$, with $x_0(n)$ and $x_{M/2}(n)$ real for M even. For the DWMT case, the modulator output would be real provided the input symbols in a block satisfy $x_{M-m-1}(n) = x_m^*(n), \quad 0 \le m \le M/2 - 1$ for M even.

The subchannel outputs are added together to produce a single output sequence $\{y(n)\}$

$$y(n) = \sum_{m=0}^{M-1} \sum_{l=-\infty}^{+\infty} x_m(l) f_m(n - lM). \tag{8}$$

The output of $W(z)$ is given by

$$r(n) = w(n) * c(n) * y(n) + w(n) * q(n). \tag{9}$$

where $\{q(n)\}$ is the channel noise sequence. The demodulator output sample in n^{th} block of m_1^{th} subchannel is given by

$$\theta_{m_1}(n) = \sum_{i=-\infty}^{+\infty} r(i) f_{m_1}'(Mn - i). \tag{10}$$

To understand the correspondence between $x_m(n)$ and $\theta_m(n)$, consider the special case where the pre-detection equalizer $W(z)$ perfectly equalizes the channel, i.e., $C(z)W(z) = z^{-\Delta}$. Let $d = KM - \Delta$ and d be non-negative. Then,

$$\theta_{m_1}(n) = x_{m_1}(n - K - p) + \text{noise term}. \tag{11}$$

Thus, with perfect pre-detection equalization, $x_{m_1}(n)$ can be estimated based on $\theta_{m_1}(n + p_1)$ only, where $p_1 = K + p$, without incorporating any other post-detection equalization.

In the general case, there will be ISI both across the subchannels and across the blocks. To mitigate the effect of ISI, we use a post-detection equalizer [2], which linearly combines the demodulator subchannel outputs to yield the estimates of the transmitted symbols. Note that in the DWMT case, the transmitted symbols in the i^{th} block are made up of the input symbols from the blocks $i, i-1, \cdots, i-p+1$. Also, the influence of an input symbol in the i^{th} block exists for blocks $i, i+1, \cdots, i+p-1$. Thus, to get an estimate of the input symbol of i_1^{th} block in the m_1^{th} subchannel, we perform the following smoothing

$$\hat{x}_{m_1}(i_1) = \sum_{k=-\nu}^{\nu} \sum_{m' \in \Omega(m_1)} \lambda_{m_1}(m', k)\theta_{m'}(i_1 + k + p_1). \tag{12}$$

In the above expression, $\Omega(m_1)$ denotes the set of indices of the subchannels that are used in the estimation of the transmitted symbols in the m_1^{th} subchannel, and ν denotes the number of blocks, prior to and after the desired block, used in the smoothing. The design of the post-detection equalizer is equivalent to choosing the parameters $\lambda_{m_1}(m', k)$ so as to minimize the contribution from the channel noise and the interfering symbols to $\hat{x}_{m_1}(i_1)$ [6].

3.2 Finite-Length Pre-detection Equalizer

The motivation for using a pre-detection equalizer is to reduce the length of the impulse response of the equalized channel. This will reduce the spread of the bases that is caused due to the channel, thereby reducing the number blocks that cause ISI. We designed this equalizer following the algorithm described in [4].

4 BLIND EQUALIZATION

Recently, a blind equalization algorithm for wavelet packet based multicarrier modulation scheme has been proposed for the case of binary PAM symbols [8]. The motivation behind the equalization in [8] is that, any channel response can be divided into a set of bands (subchannels), possibly nonuniform, where its behavior closely approximates that of a simple attenuation and delay channel. Since a wavelet packet is a narrow band sequence, a suitably designed wavelet packet would be undistorted (though attenuated) by passage through the channel. Thus, if a sequence of symbols are used to modulate a set of wavelet packets, called the carriers, then no elaborate equalization is required at the receiver (provided the wavelet packets have negligible overlap in the frequency domain). However, compensation is required for the delay introduced by the channel in each subchannel. Thus, the equalization problem essentially reduces to that of determining the delays.

4.1 Blind Equalization Algorithm for Complex Symbols Case

The wavelet packet based multicarrier modulator is as shown in Fig. 1. The receiver, consisting of the matched filters, delays and decimators (see Fig. 2), performs the role of equalizer here. The demodulator filters are related to the modulator filters by

$$H_m(z) = z^{-(pM-1)}\tilde{F}_m(z) \quad 0 \le m \le M-1, \qquad (13)$$

where p is the minimum integer that makes the filters causal.

To simplify the notation, we define $G_{mk}(z) \triangleq \tilde{H}_m(z)H_k(z)C(z)$ Then, the output of the k^{th} subchannel after equalization is given by

$$\hat{X}_k(z) = \sum_{m=0}^{M-1} X_m(z)z^{-p}\left(G_{mk}(z)z^{-\delta_k+1}\right)_{\downarrow M} + \left(Q(z)H_k(z)z^{-\delta_k}\right)_{\downarrow M} \qquad (14)$$

which can be expressed in the time domain as

$$\begin{aligned}\hat{x}_k(n) &= \sum_{m=0}^{M-1}\sum_{l=-\infty}^{+\infty} g_{mk}(Ml-\delta_k+1)x_m(n-l-p) \\ &+ \sum_{l=-\infty}^{+\infty} h_k(l)q(Mn-l-\delta_k). \qquad (15)\end{aligned}$$

If $g_{mk}(Ml-\delta_k+1) = 0$ for $k \neq m$ and some δ_k, then there will be no interchannel interference, and if $g_{kk}(Ml-\delta_k+1)$ is a delta sequence for the same δ_k, then there will be no interblock interference. The problem, therefore, is to choose δ_k. We can show [7] that

$$\begin{aligned}\max_{\delta_k} \sum_{m=0}^{M-1}\sum_{l=-\infty}^{+\infty} |g_{mk}(Ml-\delta_k+1)|^4 &= \\ \max_{\delta_k} \left(2(var[\hat{x_k}(n)])^2 - var[\hat{x_k}^2(n)]\right) \qquad (16)\end{aligned}$$

and

$$\max_{\delta_k} \sum_{m=0}^{M-1}\sum_{l=-\infty}^{+\infty} |g_{mk}(Ml-\delta_k+1)|^4 = \min_{\delta_k} var[\hat{x}_k^2(n)] \quad (17)$$

The criterion which selects δ_k as per (16) is called the maximum square variance algorithm while the one corresponding to (17) is called the minimum square variance algorithm.

In general, the channel will introduce different attenuation for different subchannels. So, for higher order symbol constellations, decision levels will be different for different subchannels. We have to know the attenuation level for each of the subchannels to set the thresholds. We choose the average power in the input symbols at the transmitter as unity. If the average power in the equalized output is normalized to unity, then the decision thresholds can be chosen from the signal space diagram corresponding to the transmitted symbol constellation.

5 SIMULATION RESULTS

We conducted computer simulations to study the performance of the DWMT system with both post-detection and blind equalization schemes. The impulse response of the channel used in the simulation is [0.227, 0.460, 0.668, 0.460, 0.227]. This channel has a linear phase and a spectral null. We have considered three cases of $|\Omega(m_1)|$ where $|\Omega(m_1)|$ denotes the size of $\Omega(m_1)$. Larger value of $|\Omega(m_1)|$ means higher complexity for the post-detection equalizer. The results (see Tables 1 and 2) show that the DWMT performs better than the DMT for all the three cases, and significantly better for $|\Omega(m_1)|$=6. This is because the DFT bases have higher spectral overlap among the subchannels, and hence, needs larger value of $|\Omega(m_1)|$ for compensating the ISI contributed from the interchannel interference. Comparing the results of Tables 2 and 3, we see that the performance with post-detection equalization is significantly better than with blind equalization. However, the performance of the blind scheme can be improved by spanning the given channel with more subchannels (see Table 4).

One way to reduce the overall bit error probability is to use nonuniform bit loading, i.e., to assign less number of bits per symbol for the poorer subchannels and more number of bits per symbol for good subchannels. The optimum assignment of bits per subchannel is described in [5]. It is found that the overall bit error probability reduces significantly by allocating different number of bits to different subchannels according to their frequency response.

6 CONCLUSIONS

In this paper, we have presented the design of complex wavelet packet bases, which constitute the orthogonal carriers for the DWMT system, and studied its performance with post-detection and blind equalization schemes. Also, we compared its performance with that of DMT.

References

[1] P. P. Vaidyanathan, *Multirate Systems and Filter Banks.* Englewood Cliffs, NJ: Prentice Hall, Inc., 1993.

[2] S. D. Sandberg and M. A. Tzannes, "Overlap Discrete Multitone Modulation for High Speed Copper Wire Communications", *IEEE J. Select. Areas Commun.*, vol. 13, no. 9, pp. 1571–1585, Dec. 1995.

[3] Yuan-Pei Lin and P. P. Vaidyanathan, "Linear Phase Cosine Modulated Maximally Decimted Filter Banks with Perfect Reconstruction", *IEEE Trans. Signal Processing*, vol. 42, no. 11, pp. 2525–2539, Nov. 1995.

[4] J. S. Chow, *Finite Length Equalization for Multi-carrier Transmission Systems*, Ph.D. Thesis, Stanford University, 1992.

[5] A. C. Bingham, "Multicarrier Modultion for Data Transmission: An Idea Whose Time Has Come", *IEEE Commun. Mag.*, pp. 5–14, May 1990.

[6] T. K. Adhikary and V. U. Reddy, "Complex Wavelet Packets for Multicarrier Modulation", *ICASSP*, May 1998.

[7] T. K. Adhikary and V. U. Reddy, "Performance of DWMT Modulation with Blind and Non-blind Equalization Schemes", *submitted to IEEE Trans. on SP*

[8] S. Gracias and V. U. Reddy, "An Equalization Algorithm for Wavelet Packet Based Modulation Schemes", *accepted for publication in IEEE Trans. Signal Processing.*

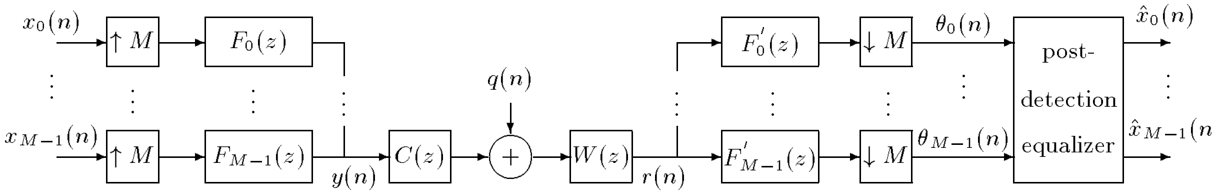

Figure 1: Discrete multicarrier modulation system

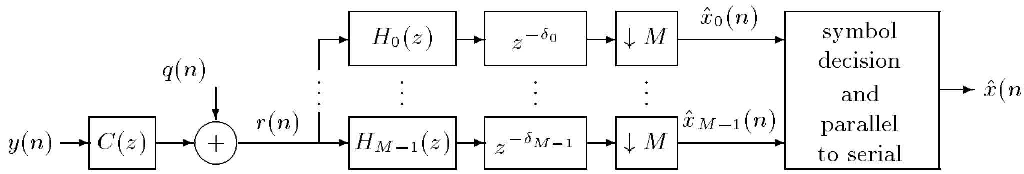

Figure 2: Receiver for blind equalization system

Table 1: Average bit error probability in each subchannel for the DMT system with post-detection equalization for 16-QAM symbol constellation (M=16)

SNR	$\|\Omega(m_1)\|$	subchannel number 0	1	2	3	4	5	6	7	8	overall value
no noise	6	0.0009	0.0071	0.0164	0.0346	0.0513	0.3540	0.2376	0.0397	0.0098	0.0933
	10	0.0001	0.0007	0.0010	0.0134	0.0092	0.3205	0.2133	0.0245	0.0017	0.0729
	16	0	0.0001	0.0002	0.0002	0.0004	0.1152	0.0274	0.0005	0.0001	0.0180
30dB	6	0.0169	0.0255	0.0804	0.0809	0.1306	0.4644	0.3666	0.1064	0.0670	0.1621
	10	0.0005	0.0051	0.0090	0.0067	0.0968	0.4504	0.3505	0.0874	0.0519	0.1290
	16	0.0004	0.0014	0.0020	0.0057	0.0797	0.4422	0.3653	0.0824	0.0341	0.1245

Table 2: Average bit error probability in each subchannel for the DWMT system with post-detection equalization for 16-QAM symbol constellation (M=16 and L_1=64)

SNR	$\|\Omega(m_1)\|$	subchannel number 0	1	2	3	4	5	6	7	overall value
no noise	6	0	0	0	0	0.0188	0.2931	0	0	0.0390
	10	0	0	0	0	0.0101	0.2788	0	0	0.0361
	16	0	0	0	0	0	0.0664	0	0	0.0083
30 dB	6	0	0	0	0	0.2903	0.4944	0.1772	0.0063	0.1210
	10	0	0	0	0	0.2913	0.4934	0.1774	0.0061	0.1210
	16	0	0	0	0	0.3067	0.4989	0.1769	0.0044	0.1234

Table 3: Average bit error probability in each subchannel for DWMT system with blind equalization for 16-QAM symbol constellation (M = 16 and L_1=64)

SNR	subchannel number 0	1	2	3	4	5	6	7	overall value
no noise	0	0	0.0033	0.0762	0.2474	0.4804	0.1395	0.0066	0.1192
30 dB	0	0	0.0042	0.0789	0.2675	0.4970	0.1774	0.0207	0.1307

Table 4: Average bit error probability in each subchannel for the DWMT system with blind equalization for 16-QAM symbol constellation (M=32 and L_1=128)

SNR	subchannel number 0	1	2	3	4	5	6	7	8	9	10	11	12	13	14	15	overall value
no noise	0	0	0	0	0	0	0	0.016	0.160	0.363	0.488	0.496	0.110	0.015	0.001	0	0.103
30dB	0	0	0	0	0	0	0.001	0.016	0.175	0.389	0.495	0.499	0.184	0.054	0.016	0.004	0.114